ETH
Eidgenössische Technische Hochschule Zürich
Swiss Federal Institute of Technology Zurich

Seminar for Applied Mathematics SAM

A mathematical and numerical framework for near-field optics

H. Ammari and D. Choi and S. Yu

Research Report No. 2018-08
March 2018

Seminar für Angewandte Mathematik
Eidgenössische Technische Hochschule
CH-8092 Zürich
Switzerland

Funding: NRF: 2016R1A2B4014530

A mathematical and numerical framework for near-field optics[*]

Habib Ammari[†] Doo Sung Choi[‡] Sanghyeon Yu[†]

Abstract

This paper is concerned with the inverse problem of reconstructing small and local perturbations of a planar surface using the field interaction between a known plasmonic particle and the planar surface. The aim is to perform a super-resolved reconstruction of these perturbations from shifts in the plasmonic frequencies of the particle-surface system. In order to analyze the interaction between the plasmonic particle and the planar surface, a well chosen conformal mapping, which transforms the particle-surface system into a coated structure, is used. Then the even Fourier coefficients of the transformed domain are related to the shifts in the plasmonic resonances of the particle-surface system. A direct reconstruction of the perturbations of the planar surface is proposed. Its viability and limitations are documented by numerical examples.

Mathematics Subject Classification (MSC2000): 35R30, 35C20.

Key words. Near-field optics, plasmonic sensing, super-resolution, Möbius transformation, generalized polarization tensors, plasmonic resonances.

1 Introduction

In conventional optical imaging and spectroscopy, a sample is typically illuminated by a light source and the scattered light is recorded by a detector. The formed images are diffraction-limited. The diffraction limit essentially means that visible light cannot image nanomaterials.

In near-field optics, by placing a probe to exploit the unique properties of metal nanostructures at optical frequencies to localize incident illumination and enhance the light-matter interaction on the sample, one breaks the resolution limit [17, 18, 19, 20, 21, 22, 29, 30]. Typically, the probe is a resonant plasmonic nanoparticle. At resonant frequencies, a light wave incident on the plasmonic probe gives rise to a greatly amplified electric field just outside the probe, which then affects the nearby sample [29, 30]. When the plasmonic

*The work of D.S. Choi is supported by the Korean Ministry of Science, ICT and Future Planning through NRF grant No. 2016R1A2B4014530.

†Department of Mathematics, ETH Zürich, Rämistrasse 101, CH-8092 Zürich, Switzerland (habib.ammari@math.ethz.ch, sanghyeon.yu@sam.math.ethz.ch).

‡Department of Mathematical Sciences, Korea Advanced Institute of Science and Technology, Daejeon 34141, South Korea (7john@kaist.ac.kr).

probe scans the sample surface one can form an image with a resolution much smaller than the diffraction limit. The physical mechanism is based on the excitation of plasmonic modes at same particular frequencies at the nanoprobe and their coupling with the evanescent light. The plasmonic particle interacts with the surface and propagates its near field information into the far-field [12, 13, 14, 29, 30]. The plasmon resonant frequency is one of the most important characterization of a plasmonic particle. It depends not only on the electromagnetic properties of the particle and its size and shape [8, 9, 26, 31], but also on the electromagnetic properties of the environment [8, 26, 28]. It is the last property which enables sensing applications of plasmonic particles [28].

In this paper, we first provide a mathematical and computational framework to elucidate physical mechanisms for going beyond this diffraction limit in near-field optics. We mathematically and numerically analyze the intriguing behavior of light under the influence of plasmonics which allows nano-sensing of samples by using a localized surface plasmonic mode at the nanoprobe. We consider a plasmonic nanoparticle placed near a locally perturbed planar surface. We propose a mathematical and numerical framework to quantitatively image the sample from shifts in the plasmonic resonances due to the coupling between the nanoparticle and the perturbed planar surface. The key idea is to use a well-chosen conformal mapping and to express the far-field and the shifts in the plasmonic resonances in terms of the Fourier coefficients of the transformed domain. We compare the reconstructed images to those obtained from the contracted generalized polarization tensors of the transformed domain, which are the gold standard in wave imaging of small particles [2, 6, 7, 10].

Our results in this work extend those in [10, 11], where a two particle system is considered. In [10, 11], the system is composed of a known plasmonic particle and a small object. By varying the relative position of the particles, it is shown that fine details of the shape of the small object can be reconstructed from the induced shifts of the plasmonic resonant frequencies of the plasmonic particle.

The paper is organized as follows. In Section 2, we provide basic results on layer potentials and then explain the concepts of plasmonic resonances and contracted generalized polarization tensors. In Section 3, we consider the forward scattering problem of the incident field interaction with a system composed of a plasmonic particle and a perturbed planar surface. We apply a Möbius transformation in order to transform the plasmonic particle and the half-plane into concentric disks. Then we derive the asymptotic expansions of the scattered field and the plasmonic resonances of the particle-surface system. In Section 4, we consider the inverse problem of reconstructing the perturbations of the planar surface. This is done by relating the the shifts in the resonances of the particle-planar surface system to the Fourier coefficients of the transformed domain. In Section 4, we provide numerical examples to justify our theoretical results and to illustrate the performances of the proposed Fourier-based reconstruction scheme. In particular, we compare the reconstructed images to those obtained from the contracted generalized polarization tensors of the transformed domain.

2 Preliminary results

2.1 Layer potentials

We recall some basic of layer potential theory that are needed for subsequent analysis. We refer to [4] for more details. We denote by $\Gamma(\mathbf{x}, \mathbf{y})$ the fundamental solution of the Laplacian in $\mathbb{R}^2$, i.e.,

$$\Gamma(\mathbf{x}, \mathbf{y}) = \frac{1}{2\pi} \ln |\mathbf{x} - \mathbf{y}|.$$

Let D be a domain $\mathbb{R}^2$ with $\mathcal{C}^{1,\eta}$ boundary for some $\eta > 0$, and let $\nu(\mathbf{x})$ be the outward normal for $Bx \in \partial D$.

The single-layer potential $\mathcal{S}_D$ associated with D is defined by

$$\mathcal{S}_D[\varphi](\mathbf{x}) = \int_{\partial D} \Gamma(\mathbf{x}, \mathbf{y})\varphi(\mathbf{y}) d\sigma(\mathbf{y}), \quad \mathbf{x} \in \mathbb{R}^2,$$

and the Neumann-Poincaré (NP) operator $\mathcal{K}_D^*$ by

$$\mathcal{K}_D^*[\varphi](\mathbf{x}) = \int_{\partial D} \frac{\partial \Gamma}{\partial \nu(\mathbf{x})}(\mathbf{x}, \mathbf{y})\varphi(\mathbf{y}) d\sigma(\mathbf{y}), \quad \mathbf{x} \in \partial D.$$

The following jump relations hold:

$$\mathcal{S}_D[\varphi]\big|_+ = \mathcal{S}_D[\varphi]\big|_-, \tag{2.1}$$

$$\frac{\partial \mathcal{S}_D[\varphi]}{\partial \nu}\Big|_\pm = (\pm\frac{1}{2}I + \mathcal{K}_D^*)[\varphi]. \tag{2.2}$$

Here, the subscripts $+$ and $-$ indicate the limits from outside and inside D, respectively.

Let $H^{1/2}(\partial D)$ be the usual Sobolev space and let $H^{-1/2}(\partial D)$ be its dual space with respect to the duality pairing $(\cdot, \cdot)_{-\frac{1}{2},\frac{1}{2}}$. We denote by $H_0^{-1/2}(\partial D)$ the collection of all $\varphi \in H^{-1/2}(\partial D)$ such that $(\varphi, 1)_{-\frac{1}{2},\frac{1}{2}} = 0$.

The NP operator is bounded from $H^{-1/2}(\partial D)$ to $H^{-1/2}(\partial D)$. Moreover, the operator $\lambda I - \mathcal{K}_D^* : L^2(\partial D) \to L^2(\partial D)$ is invertible for any $|\lambda| > 1/2$ [4, 25]. Although the NP operator is not self-adjoint on $L^2(\partial D)$, it can be symmetrized on $H_0^{-1/2}(\partial D)$ with a proper inner product [15, 8]. In fact, let $\mathcal{H}^*(\partial D)$ be the space $H_0^{-1/2}(\partial D)$ equipped with the inner product $(\cdot, \cdot)_{\mathcal{H}^*(\partial D)}$ defined by

$$(\varphi, \psi)_{\mathcal{H}^*(\partial D)} = -(\varphi, \mathcal{S}_D[\psi])_{-\frac{1}{2},\frac{1}{2}}, \tag{2.3}$$

for $\varphi, \psi \in H^{-1/2}(\partial D)$. Then using the Plemelj's symmetrization principle,

$$\mathcal{S}_D \mathcal{K}_D^* = \mathcal{K}_D \mathcal{S}_D,$$

it can be shown that the NP operator $\mathcal{K}_D^*$ is self-adjoint in $\mathcal{H}^*$ with the inner product $(\cdot, \cdot)_{\mathcal{H}^*(\partial D)}$ [15, 27]. Since $\mathcal{K}_D^*$ is also compact, it admits the following spectral decomposition in $\mathcal{H}^*$,

$$\mathcal{K}_D^* = \sum_{j=1}^{\infty} \lambda_j (\cdot, \varphi_j)_{\mathcal{H}^*} \varphi_j, \tag{2.4}$$

where λ_j are the eigenvalues of $\mathcal{K}_D^*$ and φ_j are their associated eigenfunctions. Note that $|\lambda_j| < 1/2$ for all $j \geq 1$.

2.2 Plasmonic resonance in the free space

In this subsection, we are interested in the frequency regime where plasmonic resonances occur in the free space. In such a regime, the wavelength of the incident field is much greater than the size of the plasmonic particle. To further simplify the analysis and better illustrate the main idea, we use the quasi-static approximation (by assuming the incident wavelength to be infinite) to model the interaction. More precisely, let Ω represent a plasmonic particle with permittivity ε_c embedded in the homogeneous space $\mathbb{R}^2$ with permittivity ε_m. We consider the following transmission problem with given incident field u^i which is harmonic in $\mathbb{R}^2$:

$$\begin{cases} \nabla \cdot (\varepsilon \nabla u) = 0 \qquad \text{in } \mathbb{R}^2, \\ (u - u^i)(\mathbf{x}) = O(|\mathbf{x}|^{-1}) \qquad \text{as } |\mathbf{x}| \to \infty, \end{cases} \tag{2.5}$$

where $\varepsilon = \varepsilon_c \chi(\Omega) + \varepsilon_m \chi(\mathbb{R}^2 \backslash \overline{\Omega})$, and $\chi(\Omega)$ and $\chi(\mathbb{R}^2 \backslash \overline{\Omega})$ are the characteristic functions of Ω and $\mathbb{R}^2 \backslash \overline{\Omega}$, respectively.

Problem (2.5) describes the response of the plasmonic particle Ω to the illumination u^i in the quasi-static limit.

The total field u outside of Ω can be represented by

$$u = u^i + \mathcal{S}_\Omega[\varphi]\,, \tag{2.6}$$

where the density φ satisfies the boundary integral equation

$$(\lambda I - \mathcal{K}_\Omega^*)[\varphi] = \frac{\partial u^i}{\partial \nu}\Big|_{\partial \Omega}. \tag{2.7}$$

Here, the permittivity contrast λ is given by

$$\lambda = \frac{\varepsilon_c + \varepsilon_m}{2(\varepsilon_c - \varepsilon_m)}. \tag{2.8}$$

Contrary to ordinary dielectric particles, the permittivity ε_c of the plasmonic particle has negative real parts. In fact, ε_c depends on the operating frequency ω and can be modeled by the following Drude's model

$$\varepsilon_c = \varepsilon_c(\omega) = 1 - \frac{\omega_p^2}{\omega(\omega + i\gamma)},$$

where $\omega_p > 0$ is called the plasma frequency and $\gamma > 0$ is the damping parameter. Since the parameter γ is typically very small, $\varepsilon_c(\omega)$ has a small imaginary part.

Now we discuss the plasmonic resonances. By applying the spectral decomposition (2.4) of $\mathcal{K}_\Omega^*$ to the integral equation (2.7), we obtain

$$\varphi = \sum_{j=1}^{\infty} \frac{(\frac{\partial u^i}{\partial \nu}, \varphi_j)_{\mathcal{H}^*(\partial\Omega)}}{\lambda - \lambda_j} \varphi_j.$$

Recall that λ_j are eigenvalues $\mathcal{K}_\Omega^*$ and they satisfy the condition that $|\lambda_j| < 1/2$. For $\omega < \omega_p$, $\Re\{\varepsilon_c(\omega)\}$ can take negative values. Then it holds that $|\Re\{\lambda(\omega)\}| < 1/2$. If there exists a frequency, say ω_j, such that $\lambda(\omega_j)$ is close to an eigenvalue λ_j of the NP operator and their difference is locally minimized. Provided that $(\frac{\partial u^i}{\partial \nu}, \varphi_j)_{\mathcal{H}^*(\partial\Omega)} \neq 0$, the eigenmode φ_j in (2.2) will be fully excited and it dominates over other modes. As a result, the scattered field $u - u^i$ will show a pronounced peak at the frequency ω_j. This phenomenon is called the plasmonic resonance and ω_j is called the plasmonic resonant frequency. We refer the reader to [15, 16, 8] for the details.

When Ω is an ellipse of the form

$$\Omega = \Big\{\mathbf{x} = (x_1, x_2) \in \mathbb{R}^2 : \frac{x_1^2}{a^2} + \frac{x_2^2}{b^2} \le 1\Big\},$$

for some constants a, b with $a < b$, we can compute the eigenvalues of the NP operator $\mathcal{K}_\Omega^*$ explicitly. In fact, they are given by

$$\pm\frac{1}{2}\Big(\frac{b-a}{b+a}\Big)^j, \quad j = 1, 2, 3, \cdots .$$

If $a = b$, then Ω is a circular disk of radius a. In this case, zero is the only eigenvalue.

2.3 Contracted generalized polarization tensors

In this subsection, we explain the concept of the generalized polarization tensors (GPTs) associated with a smooth bounded domain D having a permittivity ϵ_D. Let u be the solution of (2.5) and let λ_D be defined by (2.8) with ε_c replaced by ε_D. The scattered field $u - u^i$ has the following far-field behavior [4, p. 77]

$$(u - u^i)(\mathbf{x}) = \sum_{|\alpha|,|\beta|\le 1} \frac{1}{\alpha!\beta!}\partial^\alpha u^i(0) M_{\alpha\beta}(\lambda_D, D)\partial^\beta \Gamma(\mathbf{x}), \quad |\mathbf{x}| \to +\infty,$$

where $M_{\alpha\beta}(\lambda_D, D)$ is given by

$$M_{\alpha\beta}(\lambda_D, D) := \int_{\partial D} y^\beta (\lambda_D I - \mathcal{K}_D^*)^{-1}[\frac{\partial \mathbf{x}^\alpha}{\partial \nu}](\mathbf{y})\, d\sigma(\mathbf{y}), \qquad \alpha, \beta \in \mathbb{N}^2.$$

Here, the coefficient $M_{\alpha\beta}(\lambda_D, D)$ is called the *generalized polarization tensor* [4].

For $m \in \mathbb{N}$, let $P_m(\mathbf{x})$ be the complex-valued polynomial

$$P_m(\mathbf{x}) = r^m \cos m\theta + i r^m \sin m\theta, \tag{2.9}$$

with $\mathbf{x} = re^{i\theta}$ in the polar coordinates.

For n and m in $\mathbb{N}$, we define the *contracted generalized polarization tensors* (CGPTs) to be the following linear combinations of generalized polarization tensors using the homogeneous harmonic polynomials introduced in (2.9):

$$\begin{aligned}
M_{mn}^{cc}(\lambda_D, D) &= \int_{\partial D} \Re\{P_n\}(\lambda_D I - \mathcal{K}_D^*)^{-1}[\frac{\partial \Re\{P_m\}}{\partial \nu}]\, d\sigma,\\
M_{mn}^{cs}(\lambda_D, D) &= \int_{\partial D} \Im\{P_n\}(\lambda_D I - \mathcal{K}_D^*)^{-1}[\frac{\partial \Re\{P_m\}}{\partial \nu}]\, d\sigma,\\
M_{mn}^{sc}(\lambda_D, D) &= \int_{\partial D} \Re\{P_n\}(\lambda_D I - \mathcal{K}_D^*)^{-1}[\frac{\partial \Im\{P_m\}}{\partial \nu}]\, d\sigma,\\
M_{mn}^{ss}(\lambda_D, D) &= \int_{\partial D} \Im\{P_n\}(\lambda_D I - \mathcal{K}_D^*)^{-1}[\frac{\partial \Im\{P_m\}}{\partial \nu}]\, d\sigma.
\end{aligned} \tag{2.10}$$

We remark that CGPTs defined above encodes useful information about the shape of the particle D and can be used for its reconstruction. See [3, 4, 5, 7] for more details.

3 The forward problem

In this section, we consider a plasmonic nanoparticle place close to a locally perturbed planar surface. We let $\mathbb{H}_0$ to be the (unperturbed) lower half-plane

$$\mathbb{H}_0 = \{\mathbf{x} \in \mathbb{R}^2 : \mathbf{x} = (x_1, x_2), \quad x_2 < 0\}$$

with $\partial\mathbb{H}_0 = \{\mathbf{x} \in \mathbb{R}^2 : \mathbf{x} = (x_1, 0)\}$ being its boundary.

We define $\mathbb{H}_\delta$ to be a δ-perturbation of $\mathbb{H}_0$, *i.e.*, we let $h_0 \in \mathcal{C}(\partial\mathbb{H}_0)$ and $\partial\mathbb{H}_\delta$ be given by

$$\partial\mathbb{H}_\delta = \{\mathbf{x} + \delta h_0(\mathbf{x})\nu(\mathbf{x}) : \mathbf{x} \in \partial\mathbb{H}_0\},$$

where

$$\mathrm{supp}(h_0) \subset [-R, R] \quad \text{for some } R > 0. \tag{3.1}$$

Moreover, we define a plasmonic particle Ω:

$$\Omega = \{\mathbf{x} \in \mathbb{R}^2 : |\mathbf{x} - (0, d\delta)| < \delta\},$$

for some constant $d = O(1)$, where δ is the radius of the plasmonic particle and $d\delta$ is the distance between the center of Ω and $\mathbb{H}_0$.

3.1 Transmission problem in the perturbed half-space

Now, given u^i, we consider the following transmission problem:

$$\begin{cases} \nabla \cdot (\varepsilon \nabla u) = 0 \quad \text{in } \mathbb{R}^2 \setminus (\partial\mathbb{H}_\delta \cup \partial\Omega), \\ u|_+ = u|_- \quad \text{on } \partial\mathbb{H}_\delta \cup \partial\Omega, \\ \varepsilon_+ \dfrac{\partial u}{\partial \nu}\Big|_+ = \varepsilon_- \dfrac{\partial u}{\partial \nu}\Big|_- \quad \text{on } \partial\mathbb{H}_\delta, \\ \varepsilon_c \dfrac{\partial u}{\partial \nu}\Big|_+ = \varepsilon_+ \dfrac{\partial u}{\partial \nu}\Big|_- \quad \text{on } \partial\Omega, \\ (u - u^i)(\mathbf{x}) = O(|\mathbf{x}|^{-1}) \quad \text{as } |\mathbf{x}| \to \infty, \end{cases} \tag{3.2}$$

where $\varepsilon = \varepsilon_- \chi(\mathbb{H}_\delta) + \varepsilon_+ \chi(\mathbb{R}^2 \setminus (\mathbb{H}_\delta \cup \Omega)) + \varepsilon_c \chi(\Omega)$ with $\varepsilon_-, \varepsilon_+ > 0$.

Define the conformal mapping Φ, for $(x_1, x_2) \in \mathbb{R}^2$, by

$$\Phi(z) = \frac{z + i\delta\sqrt{d^2 - 1}}{z - i\delta\sqrt{d^2 - 1}}, \quad z = x_1 + ix_2.$$

Then $\mathbb{H}_\delta$ and $\mathbb{R}^2 \setminus \overline{\Omega}$ are transformed into the domains

$$D_{1,\delta} := \Phi(\mathbb{H}_\delta) \text{ and } D_2 := \Phi(\mathbb{R}^2 \setminus \overline{\Omega}) = \{|\zeta| < d + \sqrt{d^2 - 1}\}.$$

Note that the original domain $D_{1,0}$ is the unit disk as

$$D_{1,0} = \Phi(\mathbb{H}_0) = \{|\zeta| < 1\}.$$

Since $D_{1,\delta}$ is a δ-perturbation of $D_{1,0}$, there is $h \in \mathcal{C}(\partial D_{1,0})$ such that $\partial D_{1,\delta}$ is given by

$$\partial D_{1,\delta} = \{\mathbf{x} + \delta h(\mathbf{x})\nu(\mathbf{x}) : \mathbf{x} \in \partial D_{1,0}\} = \{e^{i\theta} + \delta h(\theta)e^{i\theta} : \theta \in [0, 2\pi)\}. \tag{3.3}$$

The following Fig 3.1 describes the transforming system of the whole domain.

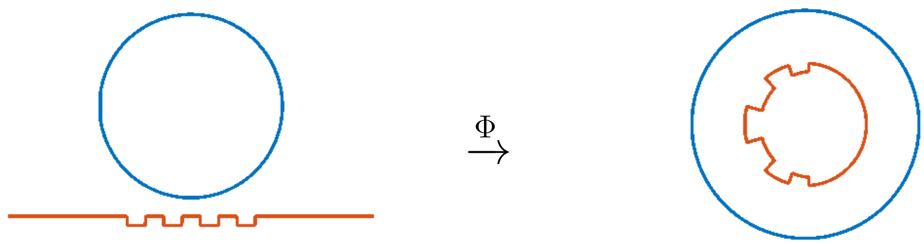

(a) h_0 perturbation on the half-plane: $\partial\mathbb{H}_\delta$ (b) h perturbation on the unit disk: $\partial D_{1,\delta}$

Figure 3.1: The plasmonic particle(left,blue) and the perturbed half-plane(left,red) are transformed into concentric perturbed disks(right).

For convenience, we denote $D_{1,\delta}$ by D_1. Then the transformed potential $\widetilde{u}(\xi) := u(\mathbf{x})$ for $\xi = \Phi(z)$ with $z = x_1 + ix_2$ satisfies the transmission problem

$$\begin{cases} \nabla \cdot (\tilde{\varepsilon}\nabla \tilde{u}) = 0 & \text{in } \mathbb{R}^2 \setminus (\partial D_1 \cup \partial D_2), \\ \tilde{u}|_+ = \tilde{u}|_- & \text{on } \partial D_1 \cup \partial D_2, \\ \varepsilon_+ \dfrac{\partial \tilde{u}}{\partial \nu_1}\Big|_+ = \varepsilon_- \dfrac{\partial \tilde{u}}{\partial \nu_1}\Big|_- & \text{on } \partial D_1, \\ \varepsilon_c \dfrac{\partial \tilde{u}}{\partial \nu_2}\Big|_+ = \varepsilon_+ \dfrac{\partial \tilde{u}}{\partial \nu_2}\Big|_- & \text{on } \partial D_2, \\ (\tilde{u} - \tilde{u}^i)(\zeta) = O(|\zeta - (1,0)|) & \text{as } \zeta \to (1,0), \end{cases}$$

where $\tilde{\varepsilon} = \varepsilon_- \chi(D_1) + \varepsilon_+ \chi(D_2 \setminus \overline{D}_1) + \varepsilon_c \chi(\mathbb{R}^2 \setminus D_2)$ and $\frac{\partial}{\partial \nu_i}$ denotes the outward normal derivative with respect to ∂D_i for $i = 1, 2$.

Since the solution $\tilde{u}$ can be represented by

$$\tilde{u} = \tilde{u}^i + \mathcal{S}_{D_1}[\phi_1] + \mathcal{S}_{D_2}[\phi_2], \tag{3.4}$$

where the densities ϕ_1 and ϕ_2 satisfy the system of integral equations

$$\begin{cases} \varepsilon_+ \dfrac{\partial}{\partial \nu_1}\Big(\tilde{u}^i + \mathcal{S}_{D_1}[\phi_1] + \mathcal{S}_{D_2}[\phi_2]\Big)\Big|_+ = \varepsilon_- \dfrac{\partial}{\partial \nu_1}\Big(\tilde{u}^i + \mathcal{S}_{D_1}[\phi_1] + \mathcal{S}_{D_2}[\phi_2]\Big)\Big|_- & \text{on } \partial D_1, \\ \varepsilon_c \dfrac{\partial}{\partial \nu_2}\Big(\tilde{u}^i + \mathcal{S}_{D_1}[\phi_1] + \mathcal{S}_{D_2}[\phi_2]\Big)\Big|_+ = \varepsilon_+ \dfrac{\partial}{\partial \nu_2}\Big(\tilde{u}^i + \mathcal{S}_{D_1}[\phi_1] + \mathcal{S}_{D_2}[\phi_2]\Big)\Big|_- & \text{on } \partial D_2, \end{cases} \tag{3.5}$$

or equivalently,

$$\begin{cases} (\lambda_{-+} I - \mathcal{K}^*_{D_1})[\phi_1] = \dfrac{\partial}{\partial \nu_1}\Big(\tilde{u}^i + \mathcal{S}_{D_2}[\phi_2]\Big) & \text{on } \partial D_1, \\ (\lambda_{+c} I - \mathcal{K}^*_{D_2})[\phi_2] = \dfrac{\partial}{\partial \nu_2}\Big(\tilde{u}^i + \mathcal{S}_{D_1}[\phi_1]\Big) & \text{on } \partial D_2, \end{cases} \tag{3.6}$$

with

$$\lambda_{-+} = \frac{\varepsilon_- + \varepsilon_+}{2(\varepsilon_- - \varepsilon_+)} \quad \text{and} \quad \lambda_{+c} = \frac{\varepsilon_+ + \varepsilon_c}{2(\varepsilon_+ - \varepsilon_c)}. \tag{3.7}$$

Since $|\lambda_{-+}| > \frac{1}{2}$ and $|\lambda_{+c}| < \frac{1}{2}$, the operator $(\lambda_{-+}I - \mathcal{K}^*_{D_1})$ is invertible. Then we have from (3.6) that

$$\phi_1 = (\lambda_{-+}I - \mathcal{K}^*_{D_1})^{-1}\frac{\partial}{\partial \nu_1}\Big(\tilde{u}^i + \mathcal{S}_{D_2}[\phi_2]\Big). \tag{3.8}$$

By substituting (3.8) into (3.6), we get the following result.

Proposition 3.1. *The density ϕ_2 on ∂D_2 satisfies the equation*

$$(\lambda_{+c}I - \mathcal{A})[\phi_2] = \frac{\partial \tilde{u}_{D_1}}{\partial \nu_2} \quad \text{on } \partial D_2,$$

where the operator $\mathcal{A}$ is given by

$$\mathcal{A} := \mathcal{K}^*_{D_2} + \frac{\partial}{\partial \nu_2}\mathcal{S}_{D_1}(\lambda_{-+}I - \mathcal{K}^*_{D_1})^{-1}\frac{\partial \mathcal{S}_{D_2}[\cdot]}{\partial \nu_1},$$

and

$$\tilde{u}_{D_1} := \tilde{u}^i + \mathcal{S}_{D_1}(\lambda_{-+}I - \mathcal{K}^*_{D_1})^{-1}\left[\frac{\partial \tilde{u}^i}{\partial \nu_1}\right].$$

3.2 Matrix representation of the operator $\mathcal{A}$

Let us now compute the operator $\mathcal{A} : \mathcal{H}^*(\partial D_2) \to \mathcal{H}^*(\partial D_2)$, where $\mathcal{H}^*(\partial D_2)$ is defined by (2.3) with D replaced by D_2. Since $\partial D_{1,0}$ is the unit circle, we use the Fourier basis $\{e^{in\theta}\}_{n\neq 0}$ as a basis of $\mathcal{H}^*(\partial D_2)$. Let (r,θ) be the polar coordinates in the ζ-plane, *i.e.*, $\zeta = re^{i\theta}$. Then the following proposition holds.

Proposition 3.2. *When $D_1 = D_{1,0}$ (i.e., for $\delta = 0$), we have for $\zeta = \left(d + \sqrt{d^2-1}\right)e^{i\theta} \in \partial D_2$,*

$$\mathcal{A}[e^{in\theta}](\zeta) = -\frac{1}{4\lambda_{-+}}\left(d - \sqrt{d^2-1}\right)^{2|n|} e^{in\theta} \quad \text{for } n \neq 0,$$

where λ_{-+} is defined by (3.7)

Proof. Since ∂D_1 and ∂D_2 are circles,

$$\mathcal{K}^*_{D_1}[e^{in\theta}] = \mathcal{K}^*_{D_2}[e^{in\theta}] = 0; \tag{3.9}$$

see, for instance, [2]. Moreover, from [1] it follows that

$$\frac{\partial}{\partial r}\mathcal{S}_B[e^{in\theta}](w) = \begin{cases} -\frac{1}{2}\left(\frac{r}{r_0}\right)^{|n|} e^{in\theta} & \text{if } |w| = r < r_0, \\ \frac{1}{2}\left(\frac{r_0}{r}\right)^{|n|} e^{in\theta} & \text{if } |w| = r > r_0, \end{cases} \tag{3.10}$$

where B is the disk centered at the origin and with radius r_0.

By using (3.9) and (3.10) (with B replaced by D_1 and D_2), we obtain

$$\mathcal{A}[e^{in\theta}](\zeta) = -\frac{1}{4\lambda_{-+}}\left(\frac{1}{d+\sqrt{d^2-1}}\right)^{2|n|} e^{in\theta} = -\frac{1}{4\lambda_{-+}}\left(d - \sqrt{d^2-1}\right)^{2|n|} e^{in\theta}.$$

$\square$

We introduce the complex contracted GPTs by

$$\mathbb{N}_{nm}^{(1)} := M_{nm}^{cc} - M_{nm}^{ss} + i(M_{nm}^{cs} + M_{nm}^{sc}), \tag{3.11}$$

$$\mathbb{N}_{nm}^{(2)} := M_{nm}^{cc} + M_{nm}^{ss} - i(M_{nm}^{cs} - M_{nm}^{sc}), \tag{3.12}$$

for $n, m \neq 0$. Here, $M_{nm}^{cc}, M_{nm}^{ss}, M_{nm}^{cs}$, and M_{nm}^{sc} are defined by (2.10).

We have the following formula for the shape perturbation of the complex GPTs [2, 3]:

$$\begin{aligned}&\mathbb{N}_{nm}^{(2)}(\lambda_{-+}, D_{1,\delta}) - \mathbb{N}_{nm}^{(2)}(\lambda_{-+}, D_{1,0})\\ &= \delta\left(\frac{\varepsilon_-}{\varepsilon_+} - 1\right)\int_{\partial D_{1,0}} h(\mathbf{x})\left[\frac{\partial u_n}{\partial \nu}\Big|_- \frac{\partial \overline{v_m}}{\partial \nu}\Big|_- + \frac{\varepsilon_+}{\varepsilon_-}\frac{\partial u_n}{\partial T}\Big|_- \frac{\partial \overline{v_m}}{\partial T}\Big|_-\right](\mathbf{x})d\sigma(\mathbf{x}) + O(\delta^2),\end{aligned}$$

where u_n and v_m are respectively the solutions to the following transmission problems:

$$\begin{cases}\Delta u = 0 & \text{in } \mathbb{R}^2 \setminus \partial D_{1,0},\\ u|_+ = u|_- & \text{on } \partial D_{1,0},\\ \varepsilon_+ \dfrac{\partial u}{\partial \nu}\Big|_- = \varepsilon_+ \dfrac{\partial u}{\partial \nu}\Big|_- & \text{on } \partial D_{1,0},\\ (u - H)(\mathbf{x}) = O(|\mathbf{x}|^{-1}) & \text{as } |\mathbf{x}| \to \infty,\end{cases} \tag{3.13}$$

and

$$\begin{cases}\Delta v = 0 & \text{in } \mathbb{R}^2 \setminus \partial D_{1,0},\\ \varepsilon_- v|_+ = \varepsilon_+ v|_- & \text{on } \partial D_{1,0},\\ \dfrac{\partial v}{\partial \nu}\Big|_- = \dfrac{\partial v}{\partial \nu}\Big|_- & \text{on } \partial D_{1,0},\\ (v - F)(\mathbf{x}) = O(|\mathbf{x}|^{-1}) & \text{as } |\mathbf{x}| \to \infty,\end{cases} \tag{3.14}$$

with $H(\mathbf{x}) = r^{|n|}e^{in\theta}$ and $F(\mathbf{x}) = r^{|m|}e^{im\theta}$. The solutions u_n and v_m of (3.13) and (3.14) can be explicitly computed. They are given by

$$u_n(\mathbf{x}) = \begin{cases}\frac{2\varepsilon_+}{\varepsilon_+ + \varepsilon_-} r^{|n|} e^{in\theta} & \text{if } |\mathbf{x}| = r < 1,\\ \left(r^{|n|} + \frac{\varepsilon_+ - \varepsilon_-}{\varepsilon_+ + \varepsilon_-} r^{-|n|}\right)e^{in\theta} & \text{if } |\mathbf{x}| = r > 1,\end{cases} \tag{3.15}$$

and

$$v_m(\mathbf{x}) = \begin{cases}\frac{2\varepsilon_-}{\varepsilon_+ + \varepsilon_-} r^{|m|} e^{-im\theta} & \text{if } |\mathbf{x}| = r < 1,\\ \left(r^{|m|} + \frac{\varepsilon_+ - \varepsilon_-}{\varepsilon_+ + \varepsilon_-} r^{-|m|}\right)e^{-im\theta} & \text{if } |\mathbf{x}| = r > 1.\end{cases} \tag{3.16}$$

Then, in view of (3.2), we obtain the following result.

Proposition 3.3. *For $n, m \neq 0$,*

$$\mathbb{N}_{nm}^{(2)}(\lambda_{-+}, D_{1,\delta}) - \mathbb{N}_{nm}^{(2)}(\lambda_{-+}, D_{1,0}) = \delta \frac{2\pi(\varepsilon_-|nm| + \varepsilon_+ nm)}{(\varepsilon_- - \varepsilon_+)\lambda_{-+}^2}\hat{h}(m-n) + O(\delta^2), \tag{3.17}$$

where λ_{-+} is defined by (3.7) and $\hat{h}(k)$ is the Fourier coefficient of $h(\theta) := h(\cos\theta, \sin\theta)$ given by

$$\hat{h}(k) = \frac{1}{2\pi}\int_0^{2\pi} h(\theta)e^{-ik\theta}d\theta.$$

Note that, since h is a real-valued function,

$$\hat{h}(-k) = \overline{\hat{h}(k)} \tag{3.18}$$

for all $k \in \mathbb{N}$.

Proposition 3.4. *When $D_1 = D_{1,\delta}$, we have for $\zeta = \left(d + \sqrt{d^2-1}\right)e^{i\theta} \in \partial D_2$,*

$$\mathcal{A}[e^{in\theta}](\zeta) = \sum_{m\in\mathbb{Z}\setminus\{0\}} -\frac{1}{8\pi|n|}\left(d - \sqrt{d^2-1}\right)^{|n|+|m|}\mathbb{N}^{(2)}_{nm}(\lambda_{-+}, D_{1,\delta})e^{im\theta} \quad \textit{for } n \neq 0.$$

Proof. Following the same arguments as those in [11], we obtain

$$\mathcal{A}[\varphi^c_n](\zeta) = \sum_{m=1}^{\infty} -\frac{1}{4\pi|n|}\left(d - \sqrt{d^2-1}\right)^{|n|+m}[M^{cc}_{nm}(\lambda_{-+}, D_{1,0})\varphi^c_m(\theta) + M^{cs}_{nm}(\lambda_{-+}, D_{1,0})\varphi^s_m(\theta)],$$

$$\mathcal{A}[\varphi^s_n](\zeta) = \sum_{m=1}^{\infty} -\frac{1}{4\pi|n|}\left(d - \sqrt{d^2-1}\right)^{|n|+m}[M^{sc}_{nm}(\lambda_{-+}, D_{1,0})\varphi^c_m(\theta) + M^{ss}_{nm}(\lambda_{-+}, D_{1,0})\varphi^s_m(\theta)],$$

for $\varphi^c_n(\theta) = \cos n\theta$, $\varphi^s_n(\theta) = \sin n\theta$, and $n \neq 0$.

By using the linearity of $\mathcal{A}$, it follows that

$$\begin{aligned}
\mathcal{A}[e^{in\theta}](\zeta) &= \mathcal{A}[\varphi^c_n](\zeta) + i\mathcal{A}[\varphi^s_n](\zeta) \\
&= \sum_{m=1}^{\infty} -\frac{1}{8\pi|n|}\left(d - \sqrt{d^2-1}\right)^{|n|+m}[\mathbb{N}^{(1)}_{nm}(\lambda_{-+}, D_{1,\delta})e^{-im\theta} + \mathbb{N}^{(2)}_{nm}(\lambda_{-+}, D_{1,\delta})e^{im\theta}] \\
&= \sum_{m\in\mathbb{Z}\setminus\{0\}} -\frac{1}{8\pi|n|}\left(d - \sqrt{d^2-1}\right)^{|n|+|m|}\mathbb{N}^{(2)}_{nm}(\lambda_{-+}, D_{1,\delta})e^{im\theta},
\end{aligned}$$

as desired. □

By combining Propositions 3.2, 3.3, and 3.4, we arrive at the following approximation of $\mathcal{A}$.

Corollary 3.5. *The operator $\mathcal{A} : \mathcal{H}^*(\partial D_2) \to \mathcal{H}^*(\partial D_2)$ can be represented by a block matrix form as follows:*

$$\begin{aligned}
\mathcal{A} &= \begin{bmatrix} D_1 & & & \\ & \ddots & & \\ & & D_n & \\ & & & \ddots \end{bmatrix} + \delta \begin{bmatrix} H_{11} & H_{12} & H_{13} & \cdots \\ H_{21} & H_{22} & H_{23} & \cdots \\ H_{31} & H_{32} & H_{33} & \cdots \\ \vdots & \vdots & \vdots & \ddots \end{bmatrix} + O(\delta^2) \\
&=: \mathcal{A}_0 + \delta\mathcal{A}_1 + O(\delta^2),
\end{aligned} \tag{3.19}$$

where

$$D_n = \begin{bmatrix} \lambda_0^{-n} & 0 \\ 0 & \lambda_0^n \end{bmatrix} \quad \textit{with } \lambda_0^k = -\frac{1}{4\lambda_{-+}}\left(d - \sqrt{d^2-1}\right)^{2|k|}, \tag{3.20}$$

and

$$H_{nm} = -\frac{n}{4\lambda_{-+}^2}\left(d - \sqrt{d^2-1}\right)^{n+m}\begin{bmatrix} 2\lambda_{-+}\hat{h}(n-m) & \hat{h}(n+m) \\ \hat{h}(-n-m) & 2\lambda_{-+}\hat{h}(m-n) \end{bmatrix}, \tag{3.21}$$

for $n, m \in \mathbb{N}$.

Note that since h is a real-valued function, the operator $\mathcal{A}_1$ in (3.19) is Hermitian. Moreover, for $k \neq 0$, note also that $\lambda_0^k (= \lambda_0^{-k})$, given by (3.20), is a double eigenvalue of $\mathcal{A}_0$, and its corresponding eigenvectors are $v_0^{\pm k}$, which represents the eigenfunction $e^{\pm ik\theta}$. Here, we define v_0^k as follows:

$$v_0^k = \begin{cases} \begin{bmatrix} 0 & \cdots & 0 & 1 & 0 & 0 & \cdots & \end{bmatrix}^T = \mathbf{e}_{2|k|-1} & \text{if } k < 0, \\ \\ \begin{bmatrix} 0 & \cdots & 0 & 0 & 1 & 0 & \cdots & \end{bmatrix}^T = \mathbf{e}_{2|k|} & \text{if } k > 0, \end{cases} \tag{3.22}$$

with $\mathbf{e}_n$ being the n-th unit vector.

Applying the standard perturbation theory [24] yields the following asymptotic expansion of the eigenvalue λ^k of $\mathcal{A}$:

$$\lambda^k = \lambda_0^k + \delta\lambda_1^k + O(\delta^2). \tag{3.23}$$

The corresponding eigenvector v^k admits the following expansion:

$$v^k = \alpha_k v_0^k + \beta_k v_0^{-k} + \delta v_1^k + O(\delta^2), \tag{3.24}$$

where v^k is a linear combination of v_0^k and v_0^{-k}.

4 The reconstruction problem

Our aim in this section is to reconstruct the Fourier coefficients of h from the perturbations of the eigenvalues of the operator $\mathcal{A}$. The following result holds.

Proposition 4.1. *Let h be the real-valued function in* (3.3). *We have*

$$\hat{h}(0) = -\frac{\lambda_{-+}(\lambda_1^k + \lambda_1^{-k})}{|k|}\left(d + \sqrt{d^2-1}\right)^{2|k|},$$

and, for $k \in \mathbb{N}, k \neq 0$,

$$|\hat{h}(2k)| = -\frac{2\lambda_{-+}^2(\lambda_1^{|k|} - \lambda_1^{-|k|})}{|k|}\left(d + \sqrt{d^2-1}\right)^{2|k|}.$$

Proof. We assume that the v^k's are all unit vectors. Since $\{v_0^l\}_{l\in\mathbb{Z}\setminus\{0\}}$ is the orthonormal basis for the eigenvector space, we set

$$v_1^k = \sum_{l\in\mathbb{Z}\setminus\{0\}} b_{kl} v_0^l, \tag{4.1}$$

where the constants b_{kl} are to be determined.

From (3.24) and (4.1), it follows that

$$1 = \langle v^k, v^k\rangle = \alpha_k^2 + \beta_k^2 + 2\delta(\alpha_k b_{kk} + \beta_k b_{-kk}) + O(\delta^2),$$

and hence, we obtain

$$\alpha_k^2 + \beta_k^2 = 1, \quad \alpha_k b_{kk} + \beta_k b_{-kk} = 0. \tag{4.2}$$

Now we want to solve the equation

$$\mathcal{A}v^k = \lambda^k v^k.$$

Using (3.19), (3.23), and (3.24), we have

$$(\mathcal{A}_0 + \delta\mathcal{A}_1)(\alpha_k v_0^k + \beta_k v_0^{-k} + \delta v_1^k) = (\lambda_0^k + \delta\lambda_1^k)(\alpha_k v_0^k + \beta_k v_0^{-k} + \delta v_1^k),$$

which yields the following equation satisfied by the first-order term v_1^k:

$$\mathcal{A}_0 v_1^k + \alpha_k \mathcal{A}_1 v_0^k + \beta_k \mathcal{A}_1 v_0^{-n} = \lambda_0^k v_1^k + \alpha_k \lambda_1^k v_0^k + \beta_k \lambda_1^k v_0^{-k}. \tag{4.3}$$

Substituting (4.1) into (4.3) and taking the inner product with v_0^l gives

$$b_{kl}\lambda_0^l + \alpha_k \langle v_0^l, \mathcal{A}_1 v_0^k\rangle + \beta_k \langle v_0^l, \mathcal{A}_1 v_0^{-k}\rangle = b_{kl}\lambda_0^k + \alpha_k \lambda_1^k \langle v_0^l, v_0^k\rangle + \beta_k \lambda_1^k \langle v_0^l, v_0^{-k}\rangle. \tag{4.4}$$

If we put $l = k, -k$ in (4.4), then

$$\alpha_k \lambda_1^k = \alpha_k \langle v_0^k, \mathcal{A}_1 v_0^k\rangle + \beta_k \langle v_0^k, \mathcal{A}_1 v_0^{-k}\rangle, \quad \beta_k \lambda_1^k = \alpha_k \langle v_0^{-k}, \mathcal{A}_1 v_0^k\rangle + \beta_k \langle v_0^{-k}, \mathcal{A}_1 v_0^{-k}\rangle. \tag{4.5}$$

If $l \notin \{k, -k\}$, then (4.4) yields

$$b_{kl} = \frac{\alpha_k \langle v_0^l, \mathcal{A}_1 v_0^k\rangle + \beta_k \langle v_0^l, \mathcal{A}_1 v_0^{-k}\rangle}{\lambda_0^k - \lambda_0^l}.$$

By using (3.21) and (4.2), we can solve (4.5) to obtain

$$\alpha_k = \left[\frac{\overline{\hat{h}(2k)}}{\overline{\hat{h}(2k)} + \hat{h}(2k)}\right]^{\frac{1}{2}}, \quad \beta_k = \mathrm{sgn}(k)\left[\frac{\hat{h}(2k)}{\overline{\hat{h}(2k)} + \hat{h}(2k)}\right]^{\frac{1}{2}},$$

and

$$\lambda_1^k = -\frac{|k|}{4\lambda_{-+}^2}\left(d - \sqrt{d^2-1}\right)^{2|k|}\left(2\lambda_{-+}\hat{h}(0) + \mathrm{sgn}(k)\cdot|\hat{h}(2k)|\right).$$

Hence, the proof of the proposition is complete. $\square$

5 Numerical examples

In this section, we present numerical example to support the theoretical results. We first note that the Fourier coefficients of h can be reconstructed from the perturbations in the eigenvalues of the operator $\mathcal{A}$ by using Proposition 4.1. Once h is reconstructed, the perturbation of the planar surface h_0 can be determined by inverting the conformal map Φ and constructing $\Phi^{-1}(D_{1,\delta})$. It is worth emphasizing that the perturbations in the eigenvalues of the operator $\mathcal{A}$ are exactly the shifts in the plasmonic resonance of the particle Ω due to its interaction with the local perturbation h_0. These shifts can be measured by varying the frequency of illumination. We refer to [11] for the details.

From Proposition 4.1, we only get even Fourier coefficients of h. Hence, in view of (3.18), we reconstruct h from the eigenvalue perturbations by

$$h_{eig}(\theta) = \sum_{k=-\frac{N}{2}}^{\frac{N}{2}} \hat{h}(2k)e^{i2k\theta} = \hat{h}(0) + 2\sum_{k=1}^{\frac{N}{2}} \Re[\hat{h}(2k)]\cos(2k\theta) - 2\sum_{k=1}^{\frac{N}{2}} \Im[\hat{h}(2k)]\sin(2k\theta).$$

We compare the reconstructed images to those obtained from the complex GPTs. Note that the perturbations in the complex GPTs can be constructed by using Proposition 3.3. Moreover, the complex GPTs can be obtained from second-order perturbations of the eigenvalues of the operator $\mathcal{A}$.

In the reconstruction of h using the complex GPTs, we truncate the Fourier series of order N and use (3.18):

$$h_{GPT}(\theta) = \sum_{k=-N}^{N} \hat{h}(k) e^{ik\theta} = \hat{h}(0) + 2\sum_{k=1}^{N} \Re[\hat{h}(k)]\cos(k\theta) - 2\sum_{k=1}^{N} \Im[\hat{h}(k)]\sin(k\theta).$$

5.1 Example 1

We set $\delta = 0.001$, $d = 1.04$, and $R = 0.4\delta$. Figure 5.1a shows the reconstruction of h. By transforming $\partial D_{1,\delta}$ to $\partial \mathbb{H}_0$ using Φ^{-1}, we get the reconstructed h_0 as shown in Figure 5.1b.

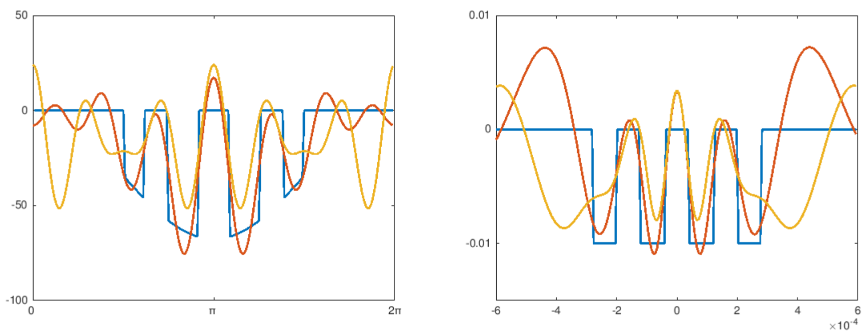

(a) Reconstruction of h (b) Reconstruction of h_0

Figure 5.1: The blue line is the true $h : [0, 2\pi] \to \mathbb{R}$, the red line is the reconstructed h from the complex GPTs, and the yellow line is the reconstructed h from the shifts in the eigenvalues. In these reconstructions $N = 8$.

5.2 Example 2

For the second example, we set $\delta = 0.001$, $d = 2$ and $R = 2\delta$. The reconstructed h is shown in Figure 5.2a. By transforming $\partial D_{1,\delta}$ to $\partial \mathbb{H}_0$ using Φ^{-1}, we finally get the reconstructed h_0 as shown in Figure 5.2b.

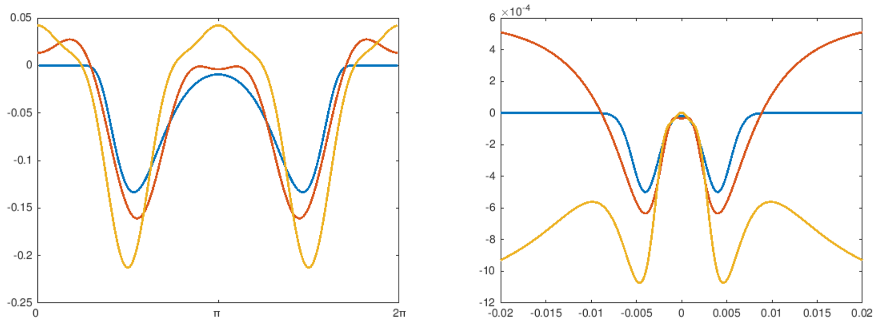

(a) Reconstruction of h

(b) Reconstruction of h_0

Figure 5.2: The blue line is a theoretical $h : [0, 2\pi] \to \mathbb{R}$, the red line is the reconstructed h using the complex GPTs, and the yellow line is the reconstructed h using the eigenvalues of $\mathcal{A}$. Here, $N = 6$.

In Figures 5.1 and 5.2, the yellow lines show very large fluctuations at both left and right extremities. This phenomenon is due to the lack of odd Fourier coefficients in h_{eig}. Nevertheless, even Fourier coefficients of h contain comprehensive information of $\partial \mathbb{H}_0$.

6 Concluding remarks

In this paper, we have introduced an original approach to recover small perturbations of a planar surface from shifts in the resonances of the plasmonic particle-surface system. Our main idea is to design a conformal mapping which transforms the particle-surface system into a coated structure, in which the inner core corresponds to the local perturbations of the planar surface. Then we have related the perturbations of the plasmonic resonances to the Fourier coefficients of the transformed perturbations. Using these (approximate) relations, we have designed a direct (non-iterative) scheme for retrieving the perturbations of the planar surface. We have shown that only even coefficients of the Fourier coefficients of the transformed perturbations can be reconstructed from the leading-order terms of the resonances. For large enough signal-to-noise ratio in the measurements, we may be able to recover both the odd coefficients and the complex GPTs from second-order terms in the resonances and therefore, achieve better resolution. This would be the subject of a forthcoming work.

References

[1] H. Ammari, G. Ciraolo, H. Kang, H. Lee, and G.W. Milton, Spectral theory of a Neumann-Poincaré-type operator and analysis of cloaking due to anomalous localized

resonance, Arch. Ration. Mech. Anal., 208 (2013), no. 2, 667–692.

[2] H. Ammari, J. Garnier, W. Jing, H. Kang, M. Lim, K. Sølna, and H. Wang, *Mathematical and Statistical Methods for Multistatic Imaging*, Lecture Notes in Mathematics, Vol. 2098, Springer, Cham, 2013.

[3] H. Ammari, J. Garnier, H. Kang, M. Lim, and S. Yu, Generalized polarization tensors for shape description, Numer. Math., 126 (2014), 199–224.

[4] H. Ammari and H. Kang, Polarization and Moment Tensors with Applications to Inverse Problems and Effective Medium Theory, Applied Mathematical Sciences, Vol. 162, Springer-Verlag, New York, 2007.

[5] H. Ammari and H. Kang, Generalized polarization tensors, inverse conductivity problems, and dilute composite materials: a review, Contemporary Mathematics, Volume 408 (2006), 1–67.

[6] H. Ammari, H. Kang, E. Kim, and J.-Y. Lee, The generalized polarization tensors for resolved imaging Part II: Shape and electromagnetic parameters reconstruction of an electromagnetic inclusion from multistatic measurements, Math. Comp., 81 (2012), 839–860.

[7] H. Ammari, H. Kang, M. Lim, and H. Zribi, The generalized polarization tensors for resolved imaging. Part I: Shape reconstruction of a conductivity inclusion, Math. Comp., 81 (2012), 367–386.

[8] H. Ammari, P. Millien, M. Ruiz, and H. Zhang, Mathematical analysis of plasmonic nanoparticles: the scalar case, Arch. Ration. Mech. Anal., 224 (2017), 597-658.

[9] H. Ammari, M. Ruiz, S. Yu, and H. Zhang, Mathematical analysis of plasmonic resonances for nanoparticles: the full Maxwell equations, J. Differential Equations, 261 (2016), 3615-3669.

[10] H. Ammari, M. Ruiz, S. Yu, and H. Zhang, Reconstructing fine details of small objects by using plasmonic spectroscopic data, SIAM J. Imaging Sci., 11 (2018), 1–23.

[11] H. Ammari, M. Ruiz, S. Yu, and H. Zhang, Reconstructing fine details of small objects by using plasmonic spectroscopic data. Part II: The strong interaction regime, arXiv:1712.02639.

[12] H. Ammari and H. Zhang, A mathematical theory of super-resolution by using a system of sub-wavelength Helmholtz resonators, Comm. Math. Phys., 337 (2015), 379–428.

[13] H. Ammari and H. Zhang, Super-resolution in high contrast media, Proc. Royal Soc. A, 2015 (471), 20140946.

[14] H. Ammari and H. Zhang, Effective medium theory for acoustic waves in bubbly fluids near Minnaert resonant frequency, SIAM J. Math. Anal., 49 (2017), 3252–3276.

[15] K. Ando and H. Kang, Analysis of plasmon resonance on smooth domains using spectral properties of the Neumann-Poincaré operator, J. Math. Anal. Appl., 435 (2016), 162–178.

[16] K. Ando, H. Kang, and H. Liu, Plasmon resonance with finite frequencies: a validation of the quasi-static approximation for diametrically small inclusions, SIAM J. Appl. Math., 76 (2016), 731–749.

[17] G. Bao, P. Li, and Y. Wang, Near-field imaging with far-field data, Appl. Math. Lett., 60 (2016), 36–42.

[18] A. Bouhelier, J. Renger, M.R. Beversluis, and L. Novotny, Plasmon-coupled tip-enhanced near-field optical microscopy, J. Microsc., 210 (2003), 220–224.

[19] P.S. Carney and J.C. Schotland, Near-field tomography. *Inside out: inverse problems and applications*, 133–168, Math. Sci. Res. Inst. Publ., 47, Cambridge Univ. Press, Cambridge, 2003.

[20] D. Courjon, *Near-Field Microscopy and Near-Field Optics*, Imperial College, 2003.

[21] N. Garcia and M. Nieto-Vesperinas, Near-field optics inverse-scattering reconstruction of reflective surfaces, Opt. Lett., 24 (1993), 2090–2092.

[22] C. Girard and A. Dereux, Near-field optics theories, Rep. Progr. Phys., 59 (1996), 657–699.

[23] J.-J. Greffet and R. Carminati, Image formation in near-field optics, Progr. Surface Sci., 56 (1997), 133–237.

[24] T. Kato, *Perturbation Theory of Linear Operators*, Springer-Verlag, 1980.

[25] O.D. Kellogg, *Foundations of Potential Theory*, Dover, New-York, 1953.

[26] K.L. Kelly, E. Coronado, L.L. Zhao, and G.C. Schatz, The optical properties of metal nanoparticles: The influence of size, shape, and dielectric environment, J. Phys. Chem. B, 107 (2003), 668–677.

[27] D. Khavinson, M. Putinar, and H.S. Shapiro, Poincaré's variational problem in potential theory, Arch. Ration. Mech. Anal., 185 (2007) 143–184.

[28] S. Link and M.A. El-Sayed, Shape and size dependence of radiative, non-radiative and photothermal properties of gold nanocrystals, Int. Rev. Phys. Chem., 19 (2000), 409–453.

[29] L. Novotny, The history of near-field optics, *Progress in Optics 50*, 137–180, E. Wolf (ed.), Elsevier, Amsterdam (2007).

[30] L. Novotny and S.J. Stranick, Near-field optical microscopy and spectroscopy with pointed probes, Ann. Rev. Phys. Chem., 57 (2006), 303–331.

[31] L.B. Scaffardi and J.O. Tocho, Size dependence of refractive index of gold nanoparticles, Nanotech., 17 (2006), 1309–1315.